TEMPORAL VARIABILITY IN THARSIS STRESS STATE BASED ON WRINKLE RIDGES AND STRIKE-SLIP FAULTING.
Chris H. Okubo[1] and Richard A. Schultz, Geomechanics–Rock Fracture Group, Department of Geological Sciences/174, Mackay School of Earth Sciences and Engineering, University of Nevada, Reno, NV 89557-0138. [1]chriso@mines.unr.edu

Introduction: Wrinkle ridges are widespread on Mars, and with a few localized exceptions, wrinkle ridge growth is generally constrained to within the L. Noachian to E. Hesperian [1,2]. Given that normal faulting and graben formation appears to have occurred throughout much of Mars' history [2], how and why was wrinkle ridge growth generally constrained to this limited period of time? In order to investigate how wrinkle ridge growth began and ended, we evaluated temporal variations in the causative near-surface stress states from chronologically-distinct sets of crosscutting thrust fault-related folds (wrinkle ridges) and strike-slip faults along the periphery of the Tharsis rise in southern Amazonis Planitia.

Tharsis strike-slip faults: Strike-slip faulting on Mars has been previously identified based on photographic evidence of strike-slip fault-related topography [3], as well as stratigraphic [4] and wrinkle ridge offsets [5]. Careful inspection of MOLA-based DEM's has revealed new evidence for strike-slip faulting on Tharsis (first noted by [6]). Strike-slip faulting results in characteristic horizontal *and* vertical displacements within the surrounding crust that have been exceedingly well quantified in studies of terrestrial analogs [7,8]. Strike-slip faults characteristically show alternating senses of slip-induced topographic subsidence within trailing quadrants of the fault, with uplift in the leading quadrants. This pattern of deformation results in a characteristic change in the sense of throw along the trace of the fault. Additionally, mechanically isolated strike-slip faults can propagate in-plane [9], resulting in linear fault traces.

Using these characteristics of surface deformation above a slipped strike-slip fault, we identify a population of strike-slip faults in southern Amazonis Planitia using MOLA-based DEM's gridded at 200 pixel/° (~279 m/pixel) resolution (**Fig. 1**) [10]. Two distinct nearly orthogonal orientations of strike-slip faults are identified. The most frequently occurring orientation, NE, is followed set of 12 faults that trend ~55°–60° east of north. The second set of faults, SE, consists of two faults that trend ~130° east of north. Measured fault lengths range from ~28 km to >350 km.

The along-strike distribution of topographic basins and rises, along with the sense of fault throw, consistently reveals right-lateral slip along the NE faults and left-lateral slip along the SE faults. Close inspection of individual fault segments in high-resolution MOC imagery shows that the thoroughgoing surface ruptures are composed of mechanically linked echelon segments, a characteristic of terrestrial strike-slip faults [11].

The mapped strike-slip faults are located at the boundary between E. Amazonian lavas and Hesperian ridged plains (**Fig. 1**) [12]. Individual Amazonian lava flows are both crosscut by the NE faults and also flow around topographic highs within the leading quadrants of the NE faults. These observations pin the date of strike-slip faulting to the E. Amazonian. Crosscutting relationships also show that slip first occurred along the more populous NE faults. Strike-slip faulting along the NE faults also extends into the older Hesperian ridged plains and crosscuts some wrinkle ridges. The Amazonian lava flows are crosscut by the SE faults and show no interaction with SE fault-related topography.

Causative stress state: What can the NE and SE sets of strike-slip faults reveal about the local stress state during the E. Amazonian? Also, could the NE and SE sets have formed within a common stress field?

The sense of displacement along a fault (thrust, normal, or strike-slip) is dictated by distinct stress states, rather than by stress magnitude alone [13]. Strike-slip faulting occurs in a stress state where the most compressive (σ_1) and least compressive (σ_3) principal stresses are horizontal, with the intermediate principal stress (σ_2) being vertical (**Fig. 2**). Two conjugate fault orientations are possible at both ±~30° from the σ_1 direction [14]. Conjugate faults have opposite slip-senses but exhibit synchronous slip. Therefore a conjugate origin for the NE and SE fault sets is inconsistent with the observed 70°–75° separation in azimuth and non-synchronous slip.

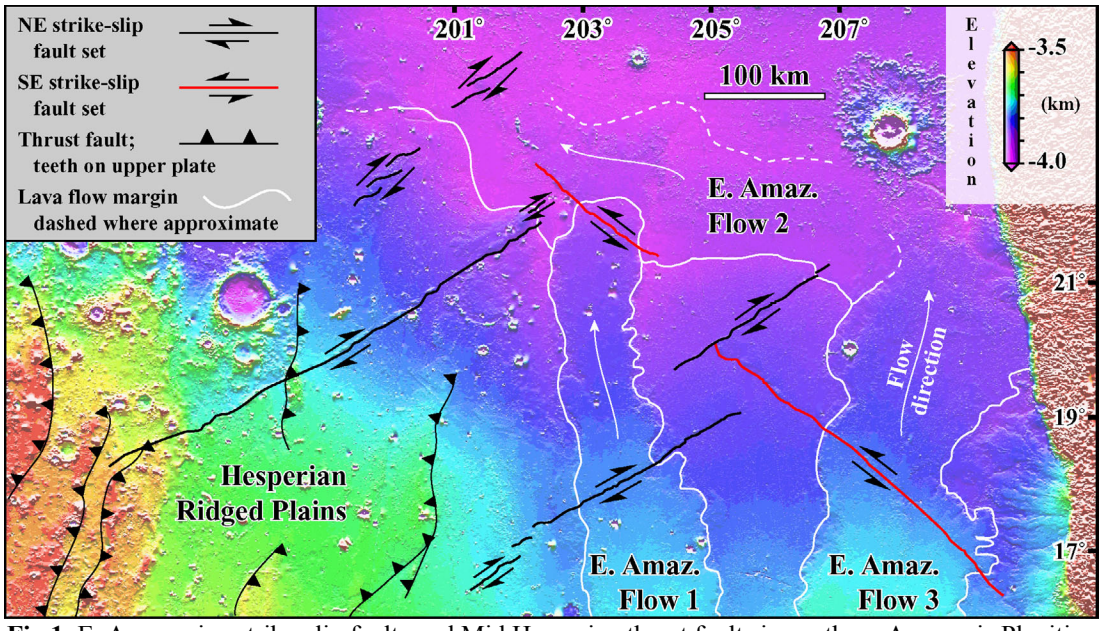

Fig 1. E. Amazonian strike-slip faults and Mid Hesperian thrust faults in southern Amazonis Planitia.

Alternatively, the NE and SE sets may have propagated under different σ_1 orientations. Assuming that the NE faults are oldest, two distinct causative stress states would require (at least) a 10°–15° *counterclockwise* rotation of σ_1 and σ_3 relative to the study area. This would imply a southerly shift in the Tharsis tectonic center since the start of the Amazonian, which is contrary to the generally northward progression of observed Tharsis tectonic centers [2].

A more tenable history for the NE and SE fault sets is revealed through numerical modeling of strike-slip faulting-induced changes in Coulomb failure stress (ΔCFS). ΔCFS is commonly used to predict localizations of secondary faults and the tendency for slip triggering of preexisting faults [15]. Observed cross-cutting relations show that slip along the NE faults was followed by slip along the SE set. Thus slip along the NE set may have led to either nucleation of the SE faults, or reactivated slip along preexisting SE-trending fractures.

The distribution of ΔCFS due to slip along a NE fault is modeled using the program COULOMB [16]. The model crust is prescribed to have a friction angle of 30°, deformation modulus of 40 GPa and density of 2700 kg/m^3. Fault length (L) and orientation is measured from the MOLA DEM. Maximum strike-slip displacement (D_{max}) is calculated from a typical D_{max}/L value for Mars of 6x10^{-3} [17]. Along-strike slip gradient of the fault is elliptical away from D_{max} at the center of the fault, transitioning to a linear taper within 0.1L of each fault tip. Slip is constant with depth. The fault is vertical and extends from the ground surface down to -12 km. The orientation of σ_1 is east-west and σ_2 is north-south, consistent with the observed sense of NE fault slip. The magnitude of σ_1 is prescribed as 30 MPa/km, with σ_3 at 7.5 MPa/km, and σ_2 being lithostatic load (ρgz = 10 MPa/km).

Our numerical model results show that the predicted orientation and slip-sense of fresh secondary faults nucleating due to NE slip are inconsistent with the observed orientation and slip-sense of the SE set. Thus nucleation of the SE faults due to NE slip can be ruled out.

Next, values of ΔCFS are resolved along a vertical plane that parallels the orientation of the SE set and intersects the slipped NE model fault. Results of this calculation show that NE slip produces magnitudes and distributions of resolved ΔCFS that enhance left-lateral slip along the SE-oriented plane. This means that slip along the NE faults is capable of inducing slip along buried, pre-existing SE-oriented fractures. Thus the SE fault set is interpreted to be the result of ΔCFS-induced slip along preexisting fractures, and that this ΔCFS is the result of displacements along the NE faults. The preexisting fractures may be related to the set of northwest-southeast trending regional joints exposed in adjacent Eumenides Dorsum.

The big picture: Our analyses show that the NE and SE faults most plausibly evolved in a common regional stress field in which the maximum horizontal compressive stress (σ_H) equals σ_1 and the minimum horizontal compressive stress (σ_h) equals σ_3. In terms of the Tharsis stress state, σ_H is radial to Tharsis, while σ_h is concentric about Tharsis.

In the study area, the transition from thrust faulting in the older adjacent Hesperian ridged plains to strike-slip faulting in the E. Amazonian lavas can be readily explained by a simple *decrease* in the magnitudes of local horizontal compressive stresses. Thrust faults form in a stress state where $\sigma_1 = \sigma_H$, $\sigma_2 = \sigma_h$, and $\sigma_3 = \rho gz = \sigma_v$ (**Fig. 2**) [13]. Thus a strike-slip stress state can be attained from a thrust fault stress state by decreasing σ_h below σ_v, while holding σ_v constant. Thus the observed sequence of younger strike-slip faults and older thrust faults in the study area reflects a decrease in the magnitude of circum-Tharsis compressional stress between the Mid Hesperian and E. Amazonian. Since the ratio of σ_1 to σ_3 is generally <~3–4 for shallow crustal rocks [18], the Tharsis-concentric stress would have been less than ~⅓–¼ of the Tharsis-radial in the E. Amazonian (with ρgz having an intermediate magnitude).

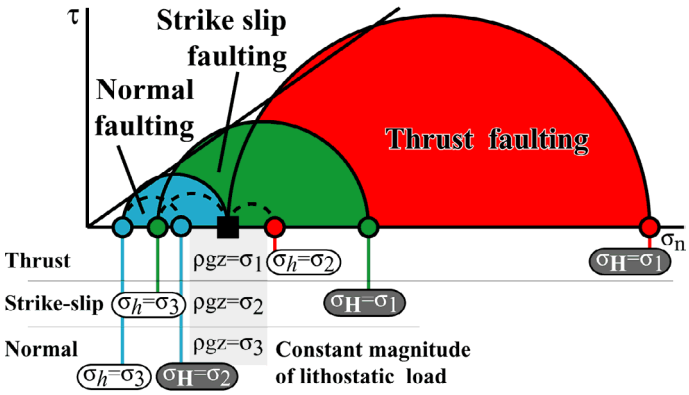

Fig 2. Stress state and corresponding sense of fault slip.

Our stress state analyses can be used to place constraints on time-dependent stress models for Tharsis. In the study area, we see evidence for a decrease in the magnitude of circum-Tharsis compressional stress. We can also see that a continued decrease in the magnitude of σ_h below that of σ_v, will result in a decrease in the magnitude of σ_H (Tharsis-radial) in order to maintain σ_1/σ_3 <~3–4. Once the magnitude of σ_H drops below σ_v (but is still compressive), then a normal faulting stress state will be reached. (Incidentally, dike-related Tharsis-radial graben formation could occur in both strike-slip and normal faulting stress states.) Alternatively, a progressive increase in Tharsis-radial and -concentric compressive stresses can cause transitions from an initial normal faulting stress state, to strike-slip, then to a thrust faulting stress state. Such an increase of Tharsis compressional stresses may be evidenced in Thaumasia, where previous work [3] has documented older strike-slip faults that are intersected by younger (E. Hesp.) wrinkle ridges (see also Artita and Schultz, this volume).

In conclusion, detailed analyses of MOLA topography reveal a strike-slip stress state following the period of wide-spread Hesperian wrinkle ridge formation. The transition from thrust faulting to strike-slip stress states indicates a decrease in the circum-Tharsis compressional stresses. Thus Tharsis-radial compressive stress was ~3–4x ρgz during the Mid Hesperian (wrinkle ridge time), but decreased to within ~1.5x ρgz by the start of the Amazonian. Throughout this transition, the magnitude of Tharsis-radial stress remains greater than that of the circum-Tharsis stress.

References: [1] Watters (1993) *JGR 98*, 17049–17060. [2] Anderson et al. (2001) *JGR 106*, 20563–20585. [3] Schultz (1989) *Nature 341*, 424–426. [4] Forsythe and Zimbelman (1988) *Nature 336*, 143–146. [5] Anguita et al. (2001) *JGR 106*, 7577–7589. [6] Tanaka et al. (2003) *JGR doi:10.1029/2002JE001908.* [7] ten Brink et al. (1996) *JGR 101*, 16205–16220. [8] Bilham and King (1989) *JGR 94*, 10204–10216. [9] Du and Aydin (1993) *GRL 20*, 1091–1094. [10] Okubo and Schultz, (2004) *Comp. & Geosci. 30*, 59–72. [11] Treiman et al. (2002) *BSSA 92*, 1171–1191. [12] Scott. and Tanaka (1986) *USGS I-1802-A*. [13] Anderson (1951) *The dynamics of faulting and dyke formation, with applications to Britain*: Oliver & Boyd, Edinburgh. [14] Jaeger and Cook (1979) *Fundamentals of Rock Mechanics*: Chapman & Hall: London. [15] King et al. (1994) *BSSA 84*, 935–953. [16] Toda et al. (1998) *JGR 103*, 24543–24565. [17] Wilkins et al. (2002) *GRL doi:10.1029/2002GL015391*. [18] Plumb (1994) *Rock Mechanics*: Balkema, Rotterdam, 71–77.

Abstract published in: Lunar and Planetary Science XXXV, CD-ROM, Lunar and Planetary Institute, Houston (2004).